Description and crystal structure of vonbezingite, a new Ca-Cu-SO₄-H₂O mineral from the Kalahari manganese field, South Africa

Yongshan Dai, George E. Harlow

Department of Mineral Sciences, The American Museum of Natural History, Central Park West at 79th Street, New York, New York 10024-5192, U.S.A.

Abstract

Vonbezingite, empirical formula $Ca_{6.03}Cu_{3.07}(SO_4)_{2.87}(OH)_{12.46} \cdot 2.06\ H_2O$, or ideally $Ca_6Cu_3(SO_4)_3(OH)_{12} \cdot 2H_2O$, space group $P2_1/c$ (pseudo-$C2/c$), $a = 15.122(2)$, $b = 14.358(1)$, $c = 22.063(4)$ Å, $\beta = 108.68(1)°$, $V = 4538.3(9)$ Å³, $Z = 8$, is a new mineral from the Wessels mine in the Kalahari manganese field of northwest Kuruman Hill, Republic of South Africa. It occurs as euhedral crystals associated with sturmanite, azurite, bultfonteinite, gypsum, calcite, barite, and other minerals. Vonbezingite is a deep azure blue and has a light blue streak, a density of 2.81 g/cm³, and a hardness (Mohs) of 4. Optically it is biaxial negative with $\alpha = 1.590(2)$, $\beta = 1.610(3)$, and $\gamma = 1.619(2)$ and strongly pleochroic, η_γ = dark blue, η_β = gray blue, and η_α = light blue. The five strongest powder diffraction lines are $3.393_x(042)$, $3.120_9(323)$, $3.188_7(043)$, $3.098_6(402)$, and $3.200_5(24\bar{2})$ Å.

The structure was solved by direct methods and refined to $R = 0.034$ using three-dimensional X-ray diffraction data: 3043 independent reflections ($F_o > 3\sigma_F$) were measured. The structure consists of thick heteropolyhedral slabs parallel to (001), in which two Ca polyhedral sheets sandwich a layer of S1 + Cu1 polyhedra. The structural slabs are bonded together by the planar layers of S2 + Cu2 polyhedra at $z \sim \frac{1}{4}$ and ¾. Vonbezingite has a superstructure of disordered S2O₄ tetrahedra based on a $C2/c$ pseudocell (b is halved), which is assumed to represent a high-temperature polymorph. H content and bonding have been modeled through coordination geometry and bond-valence sums of O atoms; the results match well with the measured density, H₂O content, and structure geometry.

Introduction

In the course of a study of minerals from the Kalahari manganese field, northwestern Cape Province, Republic of South Africa (Von Bezing et al., 1991), a conspicuous blue unidentified mineral was found. Our study has confirmed that it is a new hydrated calcium copper sulfate species, and we are pleased to name this mineral vonbezingite in honor of K. Ludi Von Bezing, a physician and mineral collector who has contributed to the mineralogy of the Kalahari manganese field. The new mineral and name have been approved by the Commission on New Minerals and Mineral Names, IMA. Type material is preserved in the American Museum of Natural History under catalogue number T100748.

Mineralogical description

Occurrence and paragenesis

Vonbezingite was found in a single solution cavity at the Wessels mine in the Kalahari manganese field, northwestern Cape Province, Republic of South Africa (Von Bezing et al., 1991). The cavity was coated with minerals including bultfonteinite, gypsum, calcite, barite, azurite, and others (Von Bezing et al., 1991) but dominated by yellowish sturmanite crystals (a Ca-Al-SO₄-H₂O mineral;

Peacor et al., 1983). Dark blue vonbezingite crystals ≤1 cm long were dispersed among the light-colored minerals lining the cavity. The mineral assemblage and texture of the aggregates suggest that the minerals crystallized from surface or ground water during a period of evaporation at ambient temperature and atmospheric pressure. During backscattered electron imaging of vonbezingite, micrometer-sized barite and azurite inclusions were discovered, which, along with the other mineral associations, indicate that the crystallizing solution was multiply saturated with respect to several oxysalts, those of Ca and sulfate being the most abundant and important.

Physical and optical properties

Vonbezingite crystals are euhedral, elongated parallel to [001], with lengths ranging from a few micrometers to 1 cm. The common forms are {110}, {010}, {100}, {111}, and {101}, and merohedral twinning on {001} is also common. Vonbezingite has a hardness of approximately 4 (Mohs scale) and is brittle with subconcoidal fracture; no cleavage or parting was observed. Density, measured on a Berman balance in toluene at room temperature, is 2.82(2) g/cm³, in excellent agreement with the calculated values of 2.81 g/cm³, based on the structure data, and

2.83 g/cm³, on the basis of the measured chemical formula.

Vonbezingite is dark blue in color, almost identical to azurite, and has a light blue streak. The luster is vitreous on fractured surfaces and subvitreous on crystal faces. Fluorescence was not observed under either long- or short-wavelength ultraviolet radiation. Optically, vonbezingite is biaxial negative, with $2V = 65(5)°$ (meas), 67° (calc), and $\alpha = 1.590(2)$, $\beta = 1.610(3)$, and $\gamma = 1.619(2)$, measured in white light. Dispersion is moderate; $r > v$. Pleochroism is strong; η_γ = dark blue, η_β = gray blue, and η_α = light blue. The crystallographic orientation of indicatrix axes is $X = b$, $Y \Lambda a = 30.2°$ and $Z \Lambda c = -11.5°$. An anomalous blue interference color is observed in all non-extinct orientations because of the dark blue color.

X-ray crystallography

Single crystals of vonbezingite were studied using precession methods and an automated Picker FACS-I four-circle diffractometer employing Mo$K\alpha$ (Zr-filtered) radiation. Preliminary film work suggested that vonbezingite is monoclinic, space group $C2/c$. However, subsequent long-exposure precession photographs of a and c axes revealed a set of very weak superstructure diffractions. These diffractions, which were verified in the intensity data obtained by diffractometer, require doubling of the b axis. By including the weak reflections and systematic absences, the final space group of vonbezingite is consistent with $P2_1/c$. The unit-cell parameters listed in Table 1 were refined without symmetry constraints using 15 reflections ($2\theta > 37°$) automatically centered on the diffractometer.

Table 2 lists the powder X-ray diffraction data obtained using an automated Philips PW1710 diffractometer with graphite-monochromated Cu$K\alpha$ radiation. The powder was slurry mounted on a glass slide with Si as an internal standard. A Gandolfi powder diffraction pattern, obtained from the single crystal used for the structure determination, matches the diffractometer data. The indexing of the powder diffractions is conformable with single-crystal diffraction data, but the weak superstructure diffractions are not observable with the powder methods so that indexing will yield $hkl_{\text{apparent cell}} = h2kl_{\text{real cell}}$ and $b_{\text{apparent cell}} = \frac{1}{2}b_{\text{real cell}}$.

Chemical composition

Vonbezingite was chemically analyzed using an ARL SEMQ nine-spectrometer electron microprobe with an operating voltage of 15 kV and a sample current of 6 nA measured on brass—the low sample current was used to minimize beam damage and H_2O loss during analysis. Except for the three major components, no elements were detected with an energy-dispersive analyzer, and no peak for elements with atomic number 9 or greater was significantly above the detection limit in wavelength-dispersive quantization, demonstrating that vonbezingite is essentially a pure Ca-Cu-SO₄ hydrate phase. Standards used for the probe analyses are kinoite (Ca, Cu), and barite (S).

TABLE 1. Crystal data and refinement details

Crystal size (mm)	0.25 × 0.25 × 0.20
Formula	$Ca_6Cu_3(SO_4)_3(OH)_{12} \cdot 2H_2O$
Space group	$P2_1/c$
Z	8
Cell parameters from least squares refinement	
a (Å)	15.122(2)
b	14.358(1)
c	22.063(4)
α (°)	90.01(1)
β	108.68(1)
γ	90.003(8)
2θ limit	1–44°
Scan type	$\theta/2\theta$
Scan width ($2\theta°$)	$2.0 \pm 0.70 \tan \theta$
Intensity standards	three per 5 h
No. data collected	5407
No. unique data	4777
No. data ($F_o > 3\sigma_F$)	3043
R	0.034
Peaks on difference map (e/Å³)	
(+)	1.3
(−)	0.98

Data were corrected for ZAF effects using Magic-IV (Colby, 1968). H_2O content was determined with a DuPont 951 thermogravimetric analyzer (TGA) with a DuPont 2100 controller and a VG Micromass 300D mass spectrometer with a mass range between 12 and 100 amu. In this mass range and up to 800 °C, H_2O was the only component recorded by the mass spectrometer. TGA reveals the following: (1) Below 310 °C the weight loss is less than 1.1%; most of this loss occurred below 110 °C and thus represents H_2O adsorbed on the sample surface. (2) From 310 to 500 °C the weight loss of 15.6% represents the release of H_2O from the sample in two steps; about 70% of the H_2O is released from 310 to 360 °C, and the remaining 30% from 430 to 500 °C. (3) From 500 to 800 °C there was no further appreciable weight loss.

Six microprobe analyses and TGA yield the composition (weight percent) of major components: CaO = 35.4 (34.9 – 35.6), CuO = 25.5 (25.2 – 25.7), SO_3 = 24.0 (23.8 – 24.3), and H_2O = 15.6 and the empirical formula $Ca_{6.03}Cu_{3.07}(SO_4)_{2.87}(OH)_{12.46} \cdot 2.06H_2O$ (based on O = 26), ideally $Ca_6Cu_3(SO_4)_3(OH)_{12} \cdot 2H_2O$. Slight deficiencies (less than 1.1%) of SO_3 in probe analyses could be attributed to minor substitution of B or C for S. Calculation of the Gladstone-Dale relationship using the constants of Mandarino (1981) yields a compatibility relation of superior agreement between optical and chemical data.

Vonbezingite is extremely similar to azurite in terms of color and morphology, as well as paragenesis. Compared to azurite, however, vonbezingite can be distinguished by its dull, earthy crystal faces, lack of cleavage, lower refraction indices, lower density, and different composition and diffraction pattern.

CRYSTAL STRUCTURE

Characterization of the new phase has revealed some interesting discoveries. In contrast to most sulfate hydrate minerals that have one or more directions of cleavage, vonbezingite has none and, thus, may represent a novel structure type. The combination of crystals with

TABLE 2. X-ray powder diffraction data

I/I_0	d_{meas} (Å)	d_{calc} (Å)	hkl	I/I_0	d_{meas} (Å)	d_{calc} (Å)	hkl
11	7.164	7.163	200	10	2.136	2.136, 2.133	$60\bar{8}, 36\bar{3}$
3	7.053	7.055	$20\bar{2}$	15	2.129	2.129	524
18	6.388	6.398	$12\bar{1}$	14	2.102	2.103	$16\bar{5}$
10	5.205	5.205	$22\bar{1}$	20	2.069	2.068, 2.069	$72\bar{3}, 44\bar{8}$
17	4.104	4.112	$32\bar{1}$	2	2.052	2.052	$72\bar{2}, 515$
23	4.094	4.097	$32\bar{2}$	4	2.046	2.045	247
37	3.974	3.976	320	4	2.029	2.031	$64\bar{1}$
35	3.964	3.934	$32\bar{3}$	7	2.017	2.018, 2.016	$72\bar{1}, 645$
25	3.786	3.779	$40\bar{2}$	2	2.005	2.010	165
16	3.756	3.758	$12\bar{5}$	2	1.969	1.968	$73\bar{3}$
23	3.663	3.671	$32\bar{4}$	4	1.954	1.950	049
100	3.393	3.395	042	12	1.948	1.948	604
55	3.368	3.363	$32\bar{5}$	6	1.942	1.941	$72\bar{7}$
13	3.349	3.355	$33\bar{3}$	13	1.907	1.905	721
9	3.295	3.293	125	12	1.903	1.901	$16\bar{7}$
7	3.286	3.286	$31\bar{6}$	5	1.898	1.897	248
5	3.238	3.242	$24\bar{1}$	12	1.878	1.876	$56\bar{2}$
53	3.200	3.199	$24\bar{2}$	19	1.867	1.867	$80\bar{2}$
65	3.188	3.191	043	17	1.863	1.864	526, 642
85	3.120	3.114	323	10	1.859	1.859	446
57	3.098	3.097	402	9	1.853	1.852	$80\bar{6}$
2	2.805	2.802	333	7	1.847	1.848	408
7	2.797	2.800	206	13	1.838	1.837	$560, 81\bar{6}$
28	2.783	2.784	$52\bar{2}$	15	1.834	1.835	$64\bar{8}$
38	2.775	2.776	$52\bar{3}$	22	1.800	1.799, 1.798	$72\bar{9}, 561$
41	2.769	2.768	$24\bar{3}, 32\bar{7}$	16	1.795	1.795	080
40	2.763	2.763	$15\bar{2}$	8	1.790	1.790	643
29	2.756	2.755	$20\bar{8}$	3	1.785	1.786	$36\bar{8}$
35	2.744	2.744, 2.743	$52\bar{1}, 245$	19	1.764	1.765	249
5	2.663	2.661	520	14	1.760	1.760	$64\bar{9}$
6	2.622	2.626	$52\bar{5}$	17	1.744	1.745	527
5	2.576	2.578, 2.575	$44\bar{3}, 244$	25	1.742	1.741	280
12	2.514	2.516, 2.512	$44\bar{4}, 32\bar{8}$	15	1.738	1.739, 1.738	$28\bar{2}, 083$
9	2.507	2.509	$60\bar{2}$	13	1.732	1.731	$56\bar{7}$
5	2.499	2.500	046	19	1.729	1.728	606
1	2.492	2.493	$41\bar{8}$	14	1.723	1.724	281
8	2.357	2.359	$16\bar{1}$	7	1.721	1.721	$28\bar{3}$
13	2.330	2.330	326	4	1.715	1.716	366
9	2.312	2.315	$44\bar{6}$	8	1.681	1.679	724
5	2.306	2.307	128	9	1.648	1.649	085
5	2.296	2.295	047	12	1.643	1.643	448
5	2.290	2.289	329	7	1.622	1.621	$48\bar{2}$
10	2.224	2.224	$52\bar{8}$	7	1.604	1.605, 1.603	$480, 76\bar{3}$
4	2.157	2.158	$36\bar{2}$	4	1.568	1.567	565
2	2.143	2.142	$70\bar{2}$	5	1.544	1.544	$48\bar{6}$

Note: Scan rate 0.6°/min.

excellent diffraction characteristics and a hydrated mineral with a complex superstructure presented us the opportunity to examine and model a variety of H-bonding arrangements, the results of which are described here.

Experimental details

A fragment of this new mineral was selected for crystal structure determination. Microscope examination under polarized light and systematic precession studies revealed that the selected crystal is untwinned and has good crystallinity, that is, sharp X-ray diffraction spots. The crystal data are given in Table 1.

Intensity data were obtained using a four-circle diffractometer for the quadrant $(+h, +k, \pm l)$ of reciprocal space, using constant precision scans with a maximum counting time of 240 s per reflection. Half of the total counting time was spent determining backgrounds on both sides of each peak. Other details of data measurement are presented in Table 1. Examination of the intensity standards showed no significant deviations in the course of data measurement (12 d). The intensity data were corrected for Lorentz and polarization effects, and absorption effects were corrected using an empirical ψ-scan technique, utilizing $\pm 180°\ \psi$ scans at 10° intervals for one reflection $(0,0,\overline{20})$. After converting the intensity data to structure factors, symmetry-equivalent reflections were averaged, yielding 4777 unique reflections, of which 3043 had $F_{obs} > 3\sigma_F$ and were used in the structure determination and refinement.

Crystallographic calculations were undertaken using the programs of the XTAL 3.0 package (both UNIX and PC versions; Hall and Stewart, 1990; Grossie, 1991). Interpolated form factors of neutral atoms, including terms for anomalous dispersion (Davenport and Hall, 1990), were used in all calculations, and all reflections were weighted equally in the least-squares refinements. Because all attempts to refine H positions were statistically invalid, the refinement procedures discussed below exclude treatment of H. Some details of the structure refinement are recorded in Table 1.

Because of the large number of atoms in the large (4538.3-Å³) unit cell ($Z = 8$) and the apparent $C2/c$ pseudocell, an initial structure solution was attempted in the b-halved pseudocell, ignoring the extremely weak reflections (k = odd). Direct methods were used for phase determination, which yielded a relative scale factor for F and an overall temperature factor based on Wilson statistics. All atoms, excluding several O atoms, were readily located on Fourier maps of electron density. Subsequent difference Fourier maps revealed that these O atoms reside in half-occupied sites, forming disordered tetrahedra around single S atoms located on the twofold axis at $(0, y, 0.25)$, special position $4e$. Full-matrix least squares refinements based on this structure model for the pseudocell converged to $R = 0.041$, with all atoms with anisotropic displacement factors. Noting the geometry of the distorted S-O tetrahedral coordination (S-O bond lengths ranging from 1.30 to 1.65 Å) and the unreasonable thermal factors ($U_{11} \gg U_{22}$ and U_{33}) of the S atom, we split S into a half-occupied $8f$ general position. The final pseudostructure refinement with this model of SO_4 disordering converged to $R = 0.039$ and resulted in a separation of 0.22 Å between the two equivalent S positions. Such a low R value indicates that the atomic arrangement in the pseudo-$C2/c$ structure is very similar to that in true $P2_1/c$ vonbezingite.

Using the positional parameters and isotropic thermal factors derived above as initial values, adjusting for the doubling of the b dimension, and shifting the origin to $(0, -0.5, 0)$, we commenced refinement of the complete set of intensity data in space group $P2_1/c$. With disordered half-occupied SO_4 units maintained, the structure could be refined only to $R = 0.168$, whereas an ordered arrangement of SO_4 units deduced from Fourier difference maps yielded a refinement with $R = 0.058$, with all atoms having isotropic displacement factors. The final full-matrix least-squares refinement converged to $R = 0.034$ and was undertaken by refining positional parameters, anisotropic temperature factors, the scale factor, and a secondary extinction factor, with a total of 686 parameters.

The positional parameters and equivalent isotropic displacement factors are given in Table 3. The atomic parameters of the pseudo-$C2/c$ structure of vonbezingite are available from the authors. Table 4 lists the selected interatomic distances and the SO_4 tetrahedral bond angles. The anisotropic displacement factors in Table 5[1] and observed and calculated structure factors in Table 6 have been submitted for deposit.

A bond-valence analysis (Brese and O'Keeffe, 1991) was used to test the site assignments. The results, Table 7, show that the cation sites are balanced with approximately integer value charges (1.91–2.23 vu for Cu^{2+} and Ca^{2+} atoms, and 5.94–6.21 vu for S^{6+}), but most O sites

---

[1] A copy of Tables 5 and 6 may be ordered as Document AM-92-509 from the Business Office, Mineralogical Society of America, 1130 Seventeenth Street NW, Suite 330, Washington, DC 20036, U.S.A. Please remit $5.00 in advance for the microfiche.

TABLE 3. Positional and isotropic displacement parameters of non-H atoms

	x	y	z	U_{eq} (Å²)
Cu1$_A$	0.2556(2)	0.8786(2)	0.5025(2)	0.0134(5)
Cu1$_B$	0.7555(2)	0.6251(2)	0.5036(1)	0.0125(5)
Cu2$_A$	0.1928(1)	0.5400(2)	0.7470(1)	0.0149(8)
Cu2$_B$	0.8221(1)	0.9648(2)	0.2536(1)	0.0161(8)
Cu2$_C$	0.6934(1)	0.7920(1)	0.7475(1)	0.0118(7)
Cu2$_D$	0.3231(1)	0.7189(1)	0.2541(1)	0.0106(7)
Ca1$_A$	0.6622(2)	0.6922(3)	0.6079(2)	0.016(1)
Ca1$_B$	0.3509(2)	0.8120(3)	0.3967(2)	0.015(1)
Ca1$_C$	1.1581(2)	0.9379(3)	0.6089(2)	0.019(1)
Ca1$_D$	−0.1550(2)	0.5582(3)	0.3942(2)	0.019(1)
Ca2$_A$	0.4481(2)	0.8632(3)	0.6459(2)	0.018(1)
Ca2$_B$	0.5557(2)	0.8622(3)	0.8550(2)	0.017(1)
Ca2$_C$	−0.0515(2)	0.8855(2)	0.1466(2)	0.017(1)
Ca2$_D$	0.0558(2)	0.8886(2)	0.3552(2)	0.017(1)
Ca3$_A$	0.2310(2)	0.6913(3)	0.6128(2)	0.016(1)
Ca3$_B$	0.7792(2)	0.8049(2)	0.3868(2)	0.013(1)
Ca3$_C$	0.7284(2)	0.9438(3)	0.6113(2)	0.022(1)
Ca3$_D$	0.2713(2)	0.5594(3)	0.3861(2)	0.022(1)
S1$_A$	0.9050(3)	0.9282(3)	0.5335(3)	0.010(2)
S1$_B$	0.1005(3)	0.5740(3)	0.4643(3)	0.011(2)
S1$_C$	0.4048(3)	0.6764(3)	0.5334(3)	0.011(2)
S1$_D$	0.6013(3)	0.8201(3)	0.4677(3)	0.010(2)
S2$_A$	0.4916(2)	1.0145(4)	0.7506(1)	0.005(2)
S2$_B$	0.0029(2)	0.7355(4)	0.2522(2)	0.018(2)
O1$_A$	0.7505(6)	0.8140(7)	0.6810(5)	0.028(3)
O1$_B$	0.2664(7)	0.6918(8)	0.3209(5)	0.032(4)
O1$_C$	0.7708(7)	0.9344(8)	0.3218(6)	0.040(4)
O1$_D$	0.2399(8)	0.5611(8)	0.6768(6)	0.047(5)
O2$_A$	0.3335(6)	0.9401(8)	0.4635(5)	0.030(4)
O2$_B$	0.6748(6)	0.5642(8)	0.5417(5)	0.031(4)
O2$_C$	0.1736(7)	0.8062(8)	0.5393(6)	0.041(4)
O2$_D$	0.8368(7)	0.6938(9)	0.4647(6)	0.039(4)
O3$_A$	0.5832(6)	0.7619(8)	0.6776(5)	0.031(4)
O3$_B$	0.4310(7)	0.7563(9)	0.3239(6)	0.041(4)
O3$_C$	1.0658(6)	0.9953(8)	0.6761(5)	0.034(4)
O3$_D$	−0.0744(7)	0.4884(8)	0.3213(6)	0.038(4)
O4$_A$	0.2051(7)	0.8210(8)	0.4183(6)	0.035(4)
O4$_B$	0.8079(7)	0.6869(8)	0.5875(6)	0.035(4)
O4$_C$	0.3078(7)	0.9381(9)	0.5861(6)	0.039(4)
O4$_D$	−0.3006(7)	0.5676(9)	0.4202(5)	0.037(4)
O5$_A$	0.3049(7)	0.9366(8)	0.3172(5)	0.035(4)
O5$_B$	0.7095(7)	0.5665(9)	0.6852(5)	0.039(4)
O5$_C$	1.2089(7)	0.8095(8)	0.6820(5)	0.032(4)
O5$_D$	0.8065(7)	0.6837(8)	0.3205(5)	0.036(4)
O6$_A$	0.8660(8)	1.0085(9)	0.6901(6)	0.049(5)
O6$_B$	0.1255(7)	0.5048(9)	0.3117(6)	0.046(4)
O6$_C$	0.3702(6)	0.7443(7)	0.6835(5)	0.025(3)
O6$_D$	0.6411(6)	0.7428(8)	0.3155(5)	0.026(3)
O7$_A$	0.4720(7)	0.5535(7)	0.4158(6)	0.049(5)
O7$_B$	0.4725(7)	1.0609(6)	0.4232(5)	0.032(4)
O7$_C$	1.0346(7)	0.696(1)	0.5881(5)	0.056(5)
O7$_D$	0.9664(6)	0.8010(8)	0.4075(5)	0.041(4)
O8$_A$	0.9964(7)	0.8810(8)	0.5507(6)	0.054(5)
O8$_B$	0.0072(8)	0.6183(9)	0.4434(6)	0.054(5)
O8$_C$	0.5103(6)	0.8729(8)	0.4492(5)	0.033(4)
O8$_D$	0.4986(6)	0.6317(7)	0.5581(5)	0.031(4)
O9$_A$	0.8462(7)	0.8917(8)	0.5666(6)	0.036(4)
O9$_B$	0.1607(7)	0.6150(9)	0.4346(6)	0.039(4)
O9$_C$	0.6644(8)	0.867(1)	0.4367(6)	0.042(4)
O9$_D$	0.3381(7)	0.6247(8)	0.5586(6)	0.033(4)
O10$_A$	0.8647(6)	0.9228(8)	0.4601(6)	0.033(4)
O10$_B$	0.1358(6)	0.5800(9)	0.5384(6)	0.036(4)
O10$_C$	0.6463(7)	0.8250(8)	0.5351(6)	0.036(4)
O10$_D$	0.3713(7)	0.6680(8)	0.4658(7)	0.040(5)
O11$_A$	0.0838(6)	0.9709(7)	0.4516(5)	0.027(4)
O11$_B$	0.0918(6)	0.4732(7)	0.4485(5)	0.026(4)
O11$_C$	0.4114(9)	0.774(1)	0.5508(7)	0.058(6)
O11$_D$	0.5825(8)	0.7238(9)	0.4489(8)	0.057(6)
O12$_A$	0.4419(5)	0.5752(6)	0.2512(4)	0.042(3)
O12$_B$	0.9447(5)	0.8195(6)	0.2509(4)	0.042(3)
O13$_A$	0.5162(6)	1.0170(6)	0.6920(4)	0.050(4)
O13$_B$	0.0258(6)	0.7349(6)	0.1923(4)	0.053(4)
O14$_A$	0.0863(6)	0.7420(7)	0.3080(4)	0.053(4)
O14$_B$	0.4257(6)	0.5141(6)	0.6923(4)	0.046(3)
O15$_A$	0.5678(6)	0.9065(6)	0.2464(4)	0.052(4)
O15$_B$	0.9506(7)	0.8496(6)	0.7556(5)	0.064(4)

TABLE 4. Selected interatomic distances (Å) and O-S-O angle (°)

Cu1$_A$ (a) -O2$_A$ (a)	1.88(1)	Cu1$_B$ (b) -O2$_B$ (b)	1.90(1)
-O4$_A$ (a)	1.95(1)	-O4$_D$ (c)	1.94(1)
-O4$_C$ (a)	1.95(1)	-O2$_D$ (b)	1.97(1)
-O2$_C$ (a)	1.98(1)	-O4$_B$ (b)	1.98(1)
-O11$_C$ (a)	2.71(1)	-O11$_B$ (a)	2.623(9)
-O11$_A$ (a)	2.811(9)	-O11$_D$ (b)	2.88(1)
Cu2$_A$ (a) -O5$_A$ (d)	1.924(9)	Cu2$_C$ (f) -O3$_A$ (f)	1.923(8)
-O1$_D$ (a)	1.92(2)	-O1$_A$ (f)	1.95(1)
-O6$_A$ (e)	1.93(2)	-O5$_D$ (i)	1.968(9)
-O3$_D$ (c)	1.98(1)	-O6$_D$ (i)	1.97(1)
Cu2$_B$ (f) -O5$_B$ (g)	1.93(1)	Cu2$_D$ (a) -O3$_B$ (a)	1.927(9)
-O6$_B$ (d)	1.94(1)	-O1$_B$ (a)	1.97(1)
-O1$_C$ (f)	1.95(1)	-O5$_C$ (j)	1.980(9)
-O3$_C$ (h)	1.982(9)	-O6$_C$ (k)	1.98(1)
-O12$_B$ (f)	2.804(9)	-O12$_A$ (a)	2.751(9)
Ca1$_A$ (f) -O4$_B$ (f)	2.39(1)	Ca1$_C$ (h) -O5$_C$ (h)	2.41(1)
-O2$_B$ (f)	2.39(1)	-O1$_C$ (f)	2.41(1)
-O5$_B$ (f)	2.43(1)	-O10$_A$ (f)	2.47(1)
-O3$_A$ (f)	2.44(1)	-O4$_C$ (a)	2.47(1)
-O10$_C$ (f)	2.45(1)	-O3$_C$ (f)	2.48(1)
-O1$_A$ (f)	2.46(1)	-O2$_C$ (a)	2.49(1)
-O8$_D$ (f)	2.517(9)	-O8$_A$ (f)	2.51(1)
Ca1$_B$ (a) -O4$_A$ (a)	2.40(1)	Ca1$_D$ (c) -O5$_D$ (b)	2.37(1)
-O2$_A$ (a)	2.42(1)	-O1$_D$ (a)	2.40(1)
-O3$_B$ (a)	2.44(1)	-O10$_B$ (a)	2.44(1)
-O5$_A$ (a)	2.44(1)	-O4$_D$ (c)	2.45(1)
-O1$_B$ (a)	2.46(1)	-O8$_B$ (c)	2.50(1)
-O8$_C$ (a)	2.476(9)	-O3$_D$ (c)	2.51(1)
-O10$_D$ (a)	2.53(1)	-O2$_D$ (b)	2.52(1)
Ca2$_A$ (f) -O11$_C$ (f)	2.37(2)	Ca2$_C$ (m) -O3$_D$ (d)	2.33(1)
-O4$_C$ (f)	2.37(1)	-O4$_B$ (g)	2.35(1)
-O6$_C$ (f)	2.37(1)	-O11$_B$ (d)	2.35(1)
-O3$_A$ (f)	2.42(1)	-O6$_B$ (d)	2.39(1)
-O7$_B$ (a)	2.47(1)	-O7$_C$ (g)	2.41(1)
-O13$_A$ (f)	2.51(1)	-O12$_B$ (f)	2.51(1)
-O12$_A$ (i)	2.52(1)	-O13$_B$ (m)	2.511(9)
Ca2$_B$ (f) -O6$_D$ (i)	2.33(1)	Ca2$_D$ (m) -O6$_A$ (h)	2.31(1)
-O11$_D$ (i)	2.33(2)	-O11$_A$ (m)	2.35(1)
-O4$_D$ (l)	2.41(1)	-O7$_D$ (f)	2.40(1)
-O7$_A$ (i)	2.44(1)	-O3$_C$ (h)	2.41(1)
-O3$_B$ (i)	2.47(1)	-O4$_A$ (m)	2.44(1)
-O14$_B$ (k)	2.47(1)	-O14$_A$ (m)	2.46(1)
-O12$_A$ (i)	2.549(8)	-O12$_B$ (f)	2.574(8)
Ca3$_A$ (a) -O2$_C$ (a)	2.28(1)	Ca3$_C$ (f) -O2$_A$ (a)	2.32(1)
-O6$_C$ (a)	2.311(9)	-O1$_A$ (f)	2.37(1)
-O1$_D$ (a)	2.32(1)	-O9$_A$ (f)	2.41(1)
-O5$_C$ (h)	2.38(1)	-O6$_A$ (f)	2.43(1)
-O10$_B$ (a)	2.41(1)	-O10$_C$ (f)	2.44(1)
-O9$_D$ (a)	2.49(1)	-O5$_A$ (a)	2.49(1)
-O7$_C$ (h)	2.84(1)	-O7$_B$ (a)	2.89(1)
Ca3$_B$ (f) -O2$_D$ (f)	2.30(1)	Ca3$_D$ (a) -O2$_B$ (b)	2.35(1)
-O1$_C$ (f)	2.33(1)	-O1$_B$ (a)	2.37(1)
-O6$_D$ (f)	2.351(9)	-O9$_B$ (a)	2.39(1)
-O5$_D$ (f)	2.39(1)	-O6$_B$ (a)	2.42(1)
-O10$_A$ (f)	2.41(1)	-O10$_D$ (a)	2.47(1)
-O9$_C$ (f)	2.50(1)	-O5$_B$ (b)	2.47(1)
-O7$_D$ (f)	2.72(1)	-O7$_A$ (a)	2.89(1)
S1$_A$ (h) -O9$_A$ (h)	1.42(1)	S1$_C$ (f) -O10$_D$ (f)	1.42(2)
-O8$_A$ (h)	1.48(1)	-O11$_C$ (f)	1.45(1)
-O11$_A$ (m)	1.48(1)	-O8$_D$ (f)	1.49(1)
-O10$_A$ (h)	1.54(1)	-O9$_D$ (f)	1.49(1)
O9$_A$ (h) ∧ O8$_A$ (h)	112.8(7)	O10$_D$ (f) ∧ O11$_C$ (f)	109.4(8)
∧ O11$_A$ (m)	107.0(8)	∧ O8$_D$ (f)	108.9(7)
∧ O10$_A$ (h)	114.9(6)	∧ O9$_D$ (f)	107.0(7)
O8$_A$ (h) ∧ O11$_A$ (m)	111.1(6)	O11$_C$ (f) ∧ O8$_D$ (f)	110.1(7)
∧ O10$_A$ (h)	105.7(8)	∧ O9$_D$ (f)	112.3(9)
O11$_A$ (m) ∧ O10$_A$ (h)	105.1(7)	O8$_D$ (f) ∧ O9$_D$ (f)	109.1(7)
S1$_B$ (c) -O9$_B$ (c)	1.41(1)	S1$_D$ (a) -O10$_C$ (a)	1.43(1)
-O8$_B$ (c)	1.48(1)	-O11$_D$ (a)	1.45(1)
-O11$_B$ (c)	1.48(1)	-O9$_C$ (a)	1.50(2)
-O10$_B$ (c)	1.55(1)	-O8$_C$ (a)	1.51(1)
O9$_B$ (c) ∧ O8$_B$ (c)	111.5(8)	O10$_C$ (a) ∧ O11$_D$ (a)	109.3(8)
∧ O11$_B$ (c)	108.6(8)	∧ O9$_C$ (a)	107.1(7)
∧ O10$_B$ (c)	114.3(7)	∧ O8$_C$ (a)	110.3(7)

TABLE 4.—CONTINUED

$O8_B$ (c) $\wedge O11_B$ (c)	110.0(6)	$O11_D$ (a) $\wedge O9_C$ (a)	113.2(9)
$\wedge O10_B$ (c)	106.1(8)	$\wedge O8_C$ (a)	108.9(7)
$O11_B$ (c) $\wedge O10_B$ (c)	106.2(7)	$O9_C$ (a) $\wedge O8_C$ (a)	108.0(7)
$S2_A$ (f) -$O13_A$ (f)	1.46(1)	$S2_B$ (m) -$O14_A$ (m)	1.456(8)
-$O15_A$ (a)	1.46(1)	-$O13_B$ (m)	1.47(1)
-$O14_B$ (k)	1.464(7)	-$O15_B$ (g)	1.47(1)
-$O12_A$ (i)	1.493(9)	-$O12_B$ (f)	1.49(1)
$O13_B$ (f) $\wedge O15_A$ (a)	110.9(6)	$O14_A$ (m) $\wedge O13_B$ (m)	111.7(6)
$\wedge O14_B$ (k)	111.9(5)	$\wedge O15_B$ (g)	110.1(6)
$\wedge O12_A$ (i)	107.5(6)	$\wedge O12_B$ (f)	108.2(6)
$O15_A$ (a) $\wedge O14_B$ (k)	109.4(5)	$O13_B$ (m) $\wedge O15_B$ (g)	109.0(6)
$\wedge O12_A$ (i)	110.6(5)	$\wedge O12_B$ (f)	107.2(6)
$O14_B$ (k) $\wedge O12_A$ (i)	106.4(5)	$O15_B$ (g) $\wedge O12_B$ (f)	110.5(6)

Note: Lower case letters in parentheses denote the symmetrical and translational operations applied: a = x,y,z (in Table 2); b = $1 - x,1 - y,1 - z$; c = $-x,1 - y,1 - z$; d = $x,3/2 - y,1/2 + z$; e = $1 - x,y - 1/2,3/2 - z$; f = $1 - x,2 - y,1 - z$; g = $1 - x,1/2 + y,3/2 - z$; h = $x - 1,y,z$; i = $1 - x,1/2 + y,1/2 - z$; j = $x - 1,3/2 - y,z - 1/2$; k = $x,3/2 - y,z - 1/2$; l = $x,1/2 + y,1/2 - z$; m = $-x,2 - y,1 - z$; n = $1 - x,y - 1/2,1/2 - z$.

are substantially underbonded, caused by the exclusion of O-H bonds from the calculation. On the basis of Pauling's electrostatic valence rule, the results of bond valence calculations were used to distinguish O atoms, OH groups, and H_2O molecules. Of the 52 O sites in the full asymmetric unit, four—$O7_X$—belong to H_2O molecules, 24—$O1_X$ through $O6_X$—to OH groups, and the rest are O atoms (X is the letter subscript of one of a set of sites that are symmetrically equivalent in the pseudo-$C2/c$ cell, listed in Table 3).

Structure description

The structure solution of vonbezingite yields an asymmetric unit with 76 non-H positions and a chemical formula $Ca_6Cu_3(SO_4)_3(OH)_{12}\cdot 2H_2O$ ($Z = 8$). The coordination chemistry of cations is typical and reasonable for oxysalt compounds. Cu atoms occupy six distinct sites, and all display coordination polyhedron distortion as a result of the Jahn-Teller effect. $Cu1_X$ atoms are coordinated by four OH groups in the equatorial plane with bond lengths of 1.89–1.97 Å and two distant O atoms at 2.62–2.88 Å in a tetragonally distorted octahedron. The $Cu2_B$ and $Cu2_D$ atoms are square planar coordinated by four OH groups plus one distant O atom. Both $Cu2_B$ and $Cu2_D$ are displaced slightly off the OH plane toward the distant O atom. $Cu2_A$ and $Cu2_C$ lie at the center of the coordination squares of four OH groups; no other oxyanions are within 3.0 Å. The 12 nonequivalent Ca atoms are sevenfold coordinated as follows:

four $Ca1_X$	5 × OH and 2 × O
four $Ca2_X$	3 × OH, 1 × H_2O, and 3 × O
four $Ca3_X$	4 × OH, 1 × H_2O, and 2 × O.

S atoms reside in six nonequivalent positions, each coordinated to four O atoms in slightly distorted tetrahedra; S-O lengths range from 1.41 to 1.55 Å, and O-S-O angles vary from 105.1 to 114.3°.

Vonbezingite can be viewed as a structure with zigzag and planar polyhedral layers parallel to (001). There are four zigzag polyhedral layers of symmetrically equivalent Ca sites at $z \sim 1/8$, $3/8$, $5/8$, and $7/8$, two zigzag layers of equivalent $Cu1_X$ and $S1_X$ polyhedra at $z \sim 0$ and $1/2$, and two nearly planar layers of equivalent $Cu2_X$ and $S2_X$ poly-

hedra at $z \sim 1/4$ and $3/4$. This arrangement is depicted in a (010) projection in Figure 1.

In the Ca polyhedral layers, alternate $Ca1_X$- and $Ca3_X$-centered polyhedra form infinite edge-sharing chains along [010] that are connected into a sheet by $Ca2_X$ polyhedra, which are linked at opposite pairs of corners between two chains (Fig. 2a), forming both three-membered and six-membered rings of Ca polyhedra. This configuration of polyhedral packing is not as dense as in many other copper and calcium sulfate minerals.

In the $Cu1_X + S1_X$ polyhedral layer (Fig. 2b), each of the $Cu1_X$ octahedra shares opposite O corners with two $S1_X$ tetrahedra, forming isolated $[Cu(OH)_4(SO_4)_2]^{6-}$ pinwheel units; the only linkages between these units within the layer are through H bonds. In each pinwheel unit, one S tetrahedron points up and the other points down, with their basal planes nearly parallel to (001), but each cross-link the sandwiching Ca layers through bonds to both basal and apical tetrahedral O atoms (Fig. 2a). Each Cu links to two OH groups in the Ca layer above and to two in the layer below, further bonding the sandwiching Ca

TABLE 7. Bond valences (vu) in the vonbezingite structure

Atom	bvs	Atom	bvs	Atom	bvs	Atom	bvs
$Cu1_A$	2.09	$S1_B$	5.96	$O4_C$	1.09	$O9_B$	2.11
B	2.06	C	6.21	D	1.08	C	1.64
$Cu2_A$	1.99	D	6.05	$O5_A$	1.06	D	1.69
B	1.97	$S2_A$	6.08	B	1.06	$O10_A$	1.83
C	1.91	B	6.04	C	1.09	B	1.82
D	1.91	$O1_A$	1.10	D	1.14	C	2.26
$Ca1_A$	2.04	B	1.08	$O6_A$	1.21	D	2.22
B	1.97	C	1.17	B	1.12	$O11_A$	1.92
C	1.91	D	1.24	C	1.19	B	1.95
D	1.96	$O2_A$	1.28	D	1.19	C	2.01
$Ca2_A$	2.06	B	1.24	$O7_A$	0.38	D	2.04
B	2.10	C	1.13	B	0.35	$O12_A$	1.93
C	2.22	D	1.11	C	0.41	B	1.93
D	2.15	$O3_A$	1.11	D	0.45	C	1.80
$Ca3_A$	2.23	B	1.05	$O8_A$	1.72	D	1.80
B	2.18	C	1.01	B	1.72	$O13_A$	1.80
C	1.97	D	1.06	C	1.62	B	1.76
D	1.95	$O4_A$	1.09	D	1.67	$O14_A$	1.85
$S1_A$	5.94	B	1.13	$O9_A$	2.05	B	1.80
						$O15_A$	1.56
						B	1.52

Note: Constants used from Brese and O'Keeffe (1991). The bonds listed in Table 4 were included in the calculations. The abbreviation bvs stands for bond valence sum.
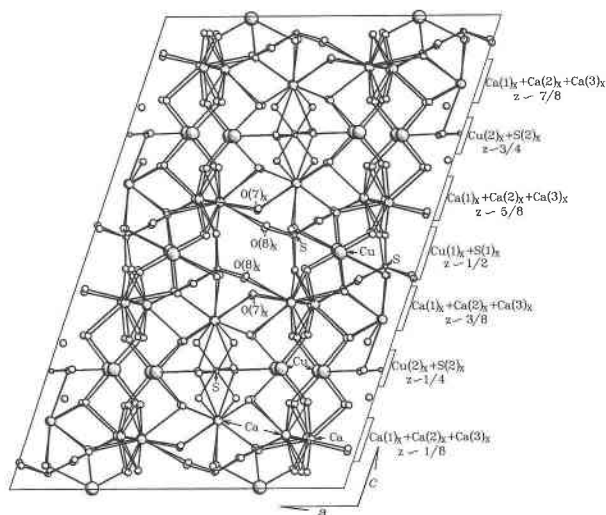
Fig. 1. The atomic arrangement of vonbezingite projected onto (010) with the cation layers indicated. The circles, from large to small, denote Cu, Ca, O, and S atoms, respectively. For clarity, only selected metal atoms are labeled and $O7_x$ and $O8_x$ sites in one structure channel are indicated.

layers together, forming complex 2 + 1 structural slabs (two Ca layers + one $Cu1_x$ + $S1_x$ layer; Fig. 1).

The final element of the sandwiched structure is a planar layer of $Cu2_x$ + $S2_x$ polyhedra (Fig. 2c). In this layer, each $Cu2_{B,D}$ pyramid shares its distant O atom with a $S2_xO_4$ tetrahedron, resulting in $[Cu(OH)_4SO_4]^{4-}$ units, but the square $Cu2_{A,C}(OH)_4$ polyhedra are not linked to other polyhedra within the layer. Bonds through H are the only connections found between the $[Cu(OH)_4SO_4]^{4-}$ units and $Cu2_{A,C}(OH)_4$ squares within the layer. The planar squares of the $Cu2_x$ polyhedra, oriented nearly perpendicular to (001), and the SO_4 tetrahedra provide strong linkage between the complex structural slabs (Fig. 1).

The structure of vonbezingite is thus constructed of Ca polyhedral sheets parallel to (001), bound together by the heteropolyhedral layers formed by $Cu1_x$ and $S1_x$ polyhedra in the form of a complex structural slab. These slabs are sandwiched by the planar $Cu2_x$ and $S2_x$ polyhedral layers at $z \sim$ ¼ and ¾, forming a three-dimensional polyhedral network. The strong three-dimensional linkage within and between the complex slabs in the structure inhibit cleavage in this mineral.

Vonbezingite represents a novel structure type relative to other Ca and Cu sulfate hydrate minerals. The sulfate hydrate minerals most similar to vonbezingite are related to devillite $[CaCu_4^{2+}(SO_4)_2(OH)_6 \cdot 3H_2O]$ (Sabelli and Zanazzi, 1972), including serpierite $[Ca(Cu^{2+},Zn)_4(SO_4)_2(OH)_6 \cdot 3H_2O]$ (Sabelli and Zanazzi, 1968), campigliaite $[Cu_4Mn^{2+}(SO_4)_2(OH)_6 \cdot 4H_2O]$ (Menchetti and Sabelli, 1982), and ktenasite $[(Cu^{2+},Zn)_5(SO_4)_2(OH)_6 \cdot 6H_2O]$ (Mellini and Merlino, 1978). The common feature of these other phases is a structure based on layers of cations octahedrally coordinated as in brucite. In the brucite-like sheets, each octahedron shares six edges with six neigh-
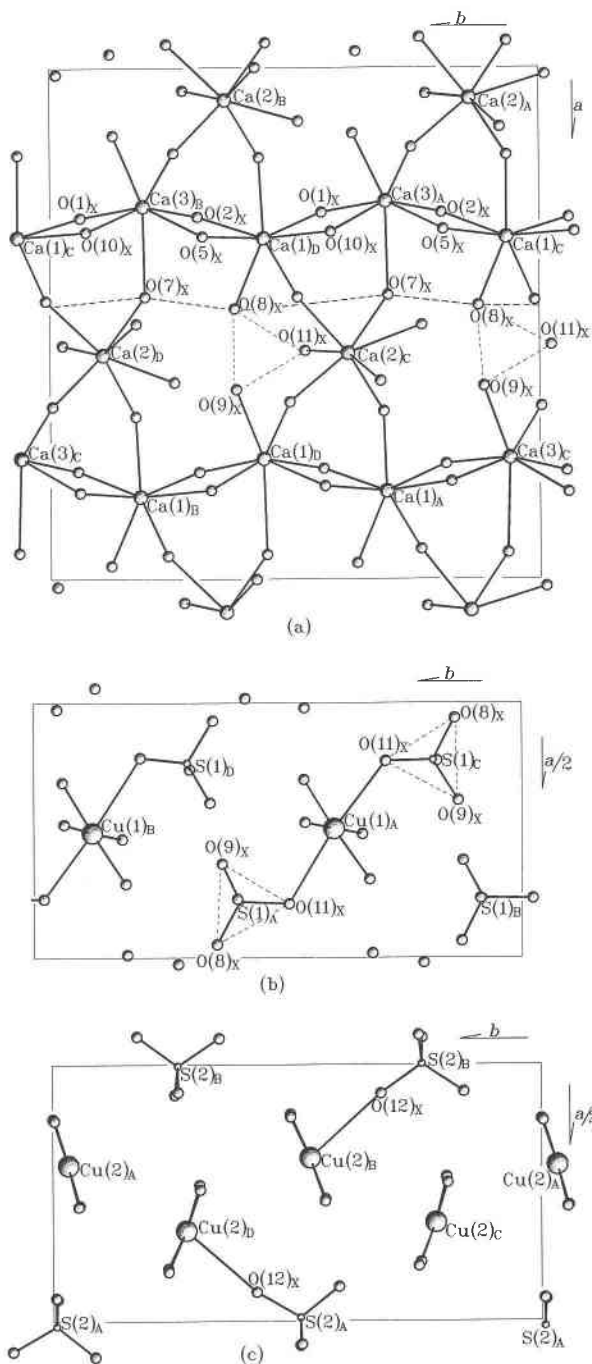

Fig. 2. Three types of polyhedral layers parallel to (001) are projected onto (001) with cation-ligand bonds indicated. (a) Ca sheet at $z \sim$ ⅛. The outlined O triangles are the basal planes of $S1O_4$ tetrahedra below this layer. The dashed line through $O7_x$ and $O8_x$ shows the projection of the H_2O chain attached to the Ca layer. (b) $Cu1_x$ + $S1_x$ layer at $z \sim$ ½ with $S1O_4$ basal triangles outlined, through which the tetrahedra are attached to the Ca layers above and below. (c) $Cu2_x$ + $S2_x$ layer at $z \sim$ ¼.

boring cation octahedra, forming a densely packed octahedral layer. Brucite-like octahedral sheets are found in many other metal sulfate hydrate minerals, such as posnjakite (Mellini and Merlino, 1979), langite (Galy et al., 1984), botallackite (Hawthorne, 1985), wroewolfeite (Hawthorne and Groat, 1985), and gerhardtite (Bovio and Locchi, 1982). The arrangement of SO_4 units and other cation polyhedra between the octahedral sheets varies among the structures, but generally the linkage between the brucite-like sheets is dominated by H bonds, resulting in the micaceous cleavage in most of these minerals. In contrast, the Ca polyhedral sheets in vonbezingite are connected by sharing corners and edges (Fig. 2a) and are not densely packed. The remaining polyhedral elements in the sheets in vonbezingite form strong connections to the adjacent layers. This three-dimensional connection of polyhedra is similar to that found in the structure of creedite ($Ca_3Al_2F_8(OH)_2(SO_4) \cdot 2H_2O$; Giuseppetti and Tadini, 1983).

H_2O molecules and H bonding

The bond valence sums of some O, OH group, and H_2O molecule sites in the structure deviate substantially from the formal valence values—2, 1, and 0, respectively—indicating H bonding that is not accounted for (Table 7). Two general rules used in modeling H bonding in hydrate structures where H positions cannot be resolved are (1) the donor (D) and acceptor (A) of a H bond do not coordinate to a single cation, and (2) the distances of D-A are generally in the range of 2.40–3.30 Å (Burn, 1970; Donnay and Allmann, 1970; Sabelli and Zanazzi, 1972; Brown, 1976; Giuseppetti and Tadini, 1983; Giester, 1989). On the basis of these rules, Table 8 lists the O-O distances in the vonbezingite structure, which may represent the presence of H bonds. By including these H bonds in the bond-valence calculation scheme of Donnay and Allmann (1970), the bond valence sums of all oxysites approach their formal valence charges, supporting the conjecture of H bonds.

Each H_2O molecule bonds to two cations ($Ca2_x$, $Ca3_x$), with $Ca2_x$-$O7_x$-$Ca3_x$ angles ranging from 121.6 to 128.8° approximately along the two lone-pair directions, and each donates two H atoms to two $O8_x$ sites, forming two H bonds with $O8_x$-$O7_x$-$O8_x$ angles varying from 95.2 to 99.9° and one D-A distance longer than the other. The "H_2O" planes defined by $O8_x$-$O7_x$-$O8_x$ are approximately perpendicular to the cation planes ($Ca2_x$-$O7_x$-$Ca3_x$). The local coordination environments around $O7_x$ are similar to those in natural and synthetic hydrate materials (Ferraris and Franchini-Angela, 1972; Chiari and Ferraris, 1982). However, the distribution of H_2O molecules in the vonbezingite structure is interesting; all the H_2O molecules are accommodated in structural channels parallel to [010] (Fig. 1). The H_2O molecules in the structure channels are linked to each other by H bonds through common acceptors ($O8_x$), forming zigzag H_2O chains in the [010] direction attached to the $Ca1_x$ and $Ca3_x$ chains in the Ca layers (Fig. 2a). This feature of channel water

TABLE 8. Selected O-O distances attributable to H bonds

$O1_A$ (f)-$O15_B$ (f)	2.99(1)	$O5_C$ (j)-$O13_B$ (a)	2.92(1)
$O1_B$ (a)-$O14_A$ (a)	2.74(1)	$O5_D$ (i)-$O15_B$ (f)	3.00(2)
$O1_C$ (f)-$O15_A$ (f)	3.01(1)	$O6_A$ (f)-$O15_B$ (f)	2.78(1)
$O1_D$ (a)-$O14_B$ (a)	2.80(1)	$O6_D$ (i)-$O15_B$ (i)	2.83(1)
$O3_A$ (f)-$O15_A$ (i)	2.90(2)	$O7_A$ (a)-$O8_D$ (b)	2.73(1)
$O3_D$ (c)-$O15_B$ (e)	2.83(2)	$O7_A$ (a)-$O8_D$ (a)	3.24(2)
$O4_A$ (a)-$O9_A$ (a)	3.08(2)	$O7_B$ (a)-$O8_C$ (a)	2.78(1)
$O4_B$ (f)-$O9_A$ (f)	3.06(2)	$O7_B$ (a)-$O8_C$ (f)	2.90(1)
$O4_C$ (a)-$O9_C$ (f)	2.90(2)	$O7_C$ (h)-$O8_A$ (h)	2.78(2)
$O4_D$ (c)-$O9_C$ (a)	2.89(2)	$O7_C$ (h)-$O8_A$ (a)	3.28(2)
$O5_A$ (a)-$O13_A$ (f)	2.86(1)	$O7_D$ (f)-$O8_B$ (m)	2.75(2)
$O5_B$ (b)-$O15_A$ (n)	2.90(2)	$O7_D$ (f)-$O8_A$ (f)	3.26(2)

Note: Lowercase letters in parentheses denote the symmetrical and translational operations applied as listed in Table 4.

in vonbezingite structure is analogous to those of many zeolite-like minerals. However, all the H_2O molecules in vonbezingite are strongly bonded to the three-dimensional polyhedral network and connected to each other by H bonds; this may have some effect on the thermal stability of this mineral.

The H bonding related to the OH groups is complex. All but eight OH groups ($O2_x$, $O3_{B,C}$, $O6_{B,C}$) are donors for H bonding; these eight OH groups do not have any other acceptors within 3.3 Å to form H bonds. No OH groups are acceptors for H bonding, largely because of the tetrahedral configuration of cations around the O atoms of OH groups. Multiple H bonds are found toward each of the $O15_x$, $O13_x$, and $O8_x$ acceptors, which are bonded only to one or two cations.

The complexity of H bonding in vonbezingite should affect its thermal stability. All of the "H_2O" in vonbezingite is bonded; there are no loose H_2O molecules. Release of either OH groups or H_2O molecules from vonbezingite requires breaking cation-O bonds, which must account for the stability of vonbezingite up to the relatively high temperature of 310 °C. The TGA analysis reveals two stages of H_2O release from the structure; the primary stage (~70% loss) from 310 to 360 °C, and a secondary one (~30% loss) from 430 to 500 °C. The OH groups account for about 75% of the mineral's H_2O content, and H_2O molecules account for 25%. The ratio of H_2O loss in the two stages suggests that the channel water molecules in vonbezingite structure may be more stable than the OH groups. This might be attributed to the complex H-bonding system in the vonbezingite structure. However, neutron diffraction refinement of the vonbezingite structure and knowledge of the high-temperature structure are needed to resolve the interpretations of the H bonding and thermal stability of vonbezingite.

The nature of the pseudostructure

The $C2/c$ pseudostructure of vonbezingite probably represents a high-temperature polymorph of $Ca_6Cu_3(SO_4)_3(OH)_{12} \cdot 2H_2O$, in which case it results from displacive disordering of $S2_xO_4$ in the $P2_1/c$ structure. The major effect of the order-disorder transition is the orientation of $S2_xO_4$ tetrahedra; the transition would have little effect

on the $Cu1_x$, $Cu2_x$, $Ca1_x$, $Ca2_x$, and $Ca3_x$ polyhedra. Thus, the transition, if it exists, should be of second order, occurring at relatively low temperature, certainly below 310 °C. The H bonding system in the crystal may be strongly affected by the disordering, because three of the four disordering O atoms are involved in the multiple H bonding.

ACKNOWLEDGMENTS

REFERENCES CITED

Bovio, B., and Locchi, S. (1982) Crystal structure of the orthorhombic basic copper nitrate, $Cu_2(OH)_3(NO_3)$. Journal of Crystallographic and Spectroscopic Research, 12, 507–517.

Brese, N.E., and O'Keeffe, M. (1991) Bond-valence parameters for solids. Acta Crystallographica, B47, 192–197.

Brown, I.D. (1976) Hydrogen bonding in perchloric acid hydrates. Acta Crystallographica, A32, 786–792.

Burn, W.H. (1970) Hydrogen. In K.H. Wedepohl, Ed., Handbook of geochemistry, p. 1-A. Springer-Verlag, New York.

Chiari, G., and Ferraris, G. (1982) The water molecule in crystalline hydrates studied by neutron diffraction. Acta Crystallographica, B38, 2331–2341.

Colby, J.W. (1968) Quantitative microprobe analysis of thin insulating films. Advances in X-Ray Analysis, 11, 287–305.

Davenport, G., and Hall, S.R. (1990) ADDREF. In S.R. Hall and J.M. Stewart, Eds., XTAL3.0 reference manual, p. 38–45. Universities of Western Australia and Maryland, Perth, Australia.

Donnay, G., and Allmann, R. (1970) How to recognize O^{2-}, OH^- and H_2O in crystal structures determined by X-rays. American Mineralogist, 55, 1003–1015.

Ferraris, G., and Franchini-Angela, M. (1972) Survey of the geometry and environment of water molecules in crystalline hydrates studied by neutron diffraction. Acta Crystallographica, B28, 3572–3583.

Galy, J., Jaud, J., Pulou, R., and Sempère, R. (1984) Structure cristalline de la langite, $Cu_4[SO_4(OH)_6H_2O] \cdot H_2O$. Bulletin de Minéralogie, 107, 641–648.

Giester, G. (1989) The crystal structures of $Ag^+Cu_2(OH)(SO_4)_2 \cdot H_2O$ and $Me^+Cu_2(OH)(SeO_4)_2 \cdot H_2O$ [Me^+ = Ag, Tl, NH_4], four new representatives of the natrochalcite type, with a note on natural natrochalcite. Zeitschrift für Kristallographie, 187, 239–247.

Giuseppetti, G., and Tadini, C. (1983) Structural analysis and refinement of Bolivian creedite, $Ca_3Al_2F_8(OH)_2(SO_4) \cdot 2H_2O$, the role of the hydrogen atoms. Neues Jahrbuch für Mineralogie Monatshefte, H2, 69–78.

Grossie, D.A. (1991) XTAL3.0 for IBM PCs and compatibles. Department of Chemistry, Wright State University, Dayton, Ohio.

Hall, S.R., and Stewart, J.M. (1990) XTAL3.0 reference manual, 408 p. Universities of Western Australia and Maryland, Perth, Australia.

Hawthorne, F.C. (1985) Refinement of the crystal structure of botallackite. Mineralogical Magazine, 49, 87–89.

Hawthorne, F.C., and Groat, L.A. (1985) The crystal structure of wroewolfeite, a mineral with $[Cu_4(OH)_6(SO_4)(H_2O)]$ sheets. American Mineralogist, 70, 1050–1055.

Mandarino, J.A. (1981) The Gladstone-Dale relationship: Part IV. The compatibility concept and its application. Canadian Mineralogist, 19, 441–450.

Mellini, M., and Merlino, S. (1978) Ktenasite, another mineral with $^2_\infty[(Cu,Zn)_2(OH)_3O]^-$ octahedral sheets. Zeitschrift für Kristallographie, 147, 129–140.

—— (1979) Posnjakite: $^2_\infty[Cu_4(OH)_6(H_2O)O]$ octahedral sheets in its structure. Zeitschrift für Kristallographie, 149, 249–257.

Menchetti, S., and Sabelli, C. (1982) Campigliaite, $Cu_4Mn(SO_4)_2(OH)_6 \cdot 4H_2O$, a new mineral from Campiglia Marittima, Tuscany, Italy. American Mineralogist, 67, 385–393.

Peacor, D.R., Dunn, P.J., and Duggan, M. (1983) Sturmanite, a ferric, boron analogue of ettringite. Canadian Mineralogist, 21, 705–709.

Sabelli, C., and Zanazzi, P.F. (1968) The crystal structure of serpierite. Acta Crystallographica, B24, 1214–1221.

—— (1972) The crystal structure of devillite. Acta Crystallographica, B28, 1182–1189.

Von Bezing, K.L., Dixon, R.D., Pohl, D., and Cavallo, G. (1991) The Kalahari manganese field: An update. Mineralogical Record, 22, 279–297.